NEW METHODOLOGIES FOR THE QUANTIFICATION OF THE CONSITUENTS OF BONE BY RAMAN SPECTROSCOPY

Karampas Ioannis, Orkoula Malvina and Kontoyannis Christos

Department of Pharmacy, University of Patras, 26500 Patras, Greece

and

Institute of Chemical Engineering and High Temperature Chemical Processes, FORTH, Patras, Greece

ABSTRACT

Bone is a composite material consisting of inorganic material (biological apatite), embedded in an organic matrix (collagen type I). Both functionality and integrity of bone are related to those constituents. The mineral gives bone tissue mechanical strength while collagen is responsible for its elasticity. Pathological conditions like osteoporosis, osteopetrosis, osteomalacia are related chemical composition changes of the tissue. In the current study, an attempt was made to quantify both mineral and organic component simultaneously in a fast and accurate way, by employing Raman Spectroscopy. Two approaches were followed: one using peak ratios and a second implementing chemometric analysis. Results showed that calibration models based on ratios of the 961 cm^{-1} vibration for apatite to the 1667 cm^{-1} for collagen and the chemometric analysis of the obtained spectra exhibited similar ability of prediction but chemometric model was characterized by superior accuracy.

INTRODUCTION

Bone is a composite material constituting by two main phases, the bone mineral which is an inorganic material resembling geological hydroxyapatite [$Ca_5(PO_4)_3(OH)$] (usually called biological apatite, BAP) and the organic matrix which is collagen I [1]. Additionally, there is also a small fraction of non collagenous proteins and lipids plus 8-10% w/w absorbed water. Many bone diseases like osteoporosis, ostepetrosis and osteomalacia are characterized by changes in the composition of BAP and/or collagen. Therefore, knowledge of the bone mineral to collagen ratio is of outmost importance for diagnostic reasons [1-3].

Many analytical techniques have been employed for the study of bone: X-ray Diffraction, X-ray Absorption, chemical analysis. Vibrational spectroscopic techniques (Infrared Absorption and Raman Scattering) have been used for the identification of apatite and collagen in bone [4]. The lack of sample pretreatment for analysis by Raman spectroscopy renders it a promising technique for the in vivo analysis of bone and consequently a diagnostic tool for many diseases [5, 6].

The scope of the present work is the construction of a calibration model based on biological apatite and collagen chemically extracted from bone to be used for the quantification of constituents in healthy as well as pathological bones.

MATERIALS AND METHODS

Isolation of BAP and collagen from bovine bone samples

Bovine bones were cut to small parallelepiped pieces 1.0cmx0.5cmx0.2cm in dimensions. Lipids and proteins were removed by immersion of samples in a 1:1 methanol-chloroform mixture, according to a delipidization protocol [7, 8]. Apatite was isolated by treatment of hydrazine as proposed by Termine et. al [9], while collagen was obtained after BAP dissolution in EDTA [10-13]. Both collagen and BAP extracted from bones were characterized by X-ray powder Diffraction, Raman and IR spectroscopy.

Pulverization of samples was accomplished in a cryogenic mill (6750 Freezer/Mill). Binary mixtures ranging from 60 to 95% w/w in BAP, were prepared by careful weighing of proper amounts and manual mixing.

Instrumentation

Raman spectra were recorded with a FRA 106/S FT-Raman (Bruker) instrument with the following characteristics: The laser excitation line used was the 1064 nm line of a Nd:YAG laser. A secondary filter was used to remove the Rayleigh line. The scattered light was collected at an angle of 180^{o} (backscattering). The system was equipped with a LN_2-cooled Ge detector (D 418). The power of the incident laser was 400 mW on sample's surface. The recorded region of all the spectra was 20-4000 cm^{-1} and for every sample six repetitive spectra were acquired, each one being the average of 200 scans. Finally, typical spectral resolution was 4 cm^{-1}.

Collection of spectra was done while the sample was rotating using a home-made system. Thus, heating of the sample was avoided while the collected signal represented the average of a much larger sample area eliminating the effect of local inhomogeneities.

RESULTS AND DISCUSSION

The intensity of a Raman line depends on a number of factors including incident laser power, frequency of scattered radiation, absorptivity of the materials involved in the scattering and the response of the detection system. Thus, the intensity of the Raman peak (absolute or integrated, A), $I(v)$, can be represented as [14]:

$$I^{v}=I_{o}K^{v}C \quad \text{or} \quad A^{v}=I_{o}K^{v}C \quad (1)$$

where I_0 is the intensity of the excitation laser line, v the Raman shift, and $K(v)$ a factor which includes the frequency-dependent terms: the overall spectrophotometer response, the self-absorption of the medium and the molecular scattering properties; C is the concentration of the Raman active species.

Thus, the concentration ratio of two components A and B of a mixture is linearly related to the ratio of the intensities of their characteristic peaks at i and j wavenumber respectively:

$$\frac{I_A^i}{I_B^j} = \frac{K_A^i}{K_B^j} \times \frac{C_A}{C_B} \quad (2)$$

The Raman spectra of BAP and collagen as well as a typical artificially made mixture are presented in Fig. 1. The spectrum of the mixture is dominated by one intense peak at 961 cm^{-1} attributed to the symmetric stretching mode of PO_4^{3-} of BAP, and another one at 2937 cm^{-1} which belongs to the vibration of (v-CH_2) of collagen [15]. Therefore, these two peaks are suitable for the quantification of BAP and collagen.

The peak at 1667 cm^{-1} (Fig 1), ascribed to amide I, can be also used for collagen quantification. In this way interference from organic impurities still remaining after the dilipidization protocol, can be avoided. In this study, calibration curves taking into consideration both collagen vibrations (1667 cm^{-1} and 2937 cm^{-1}) and the 961 cm^{-1} peak for BAP using either absolute intensities or the integrated peak areas, were constructed.

The vibration at 961 cm^{-1} (Fig 2) is overlapping with a peak at 920 cm^{-1} which corresponds to the *v(C-N)* vibration of proline (amino-acid of collagen) [15]. Consequently, the integrated area corresponds to the sum of areas of these two peaks.

Similarly, the peak intensity is the sum of two intensities, namely:

$$I^{961} = I_{BAP}^{961} + I_{COL}^{961} \qquad \text{and} \qquad A^{961} = A_{BAP}^{961} + A_{COL}^{961} \quad (3)$$

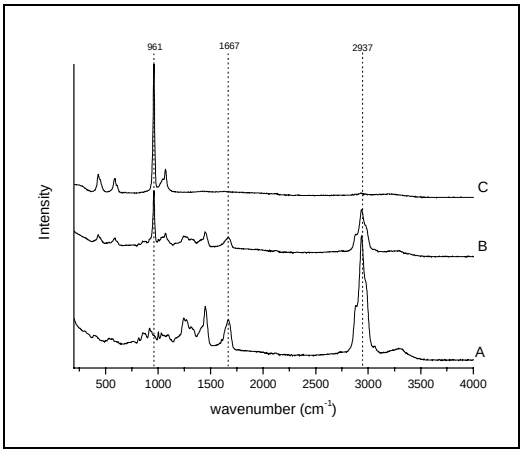

Figure 1. Raman spectra of: (A) Collagen, (B) 70/30 mixture of BAP/Col, (C) BAP.

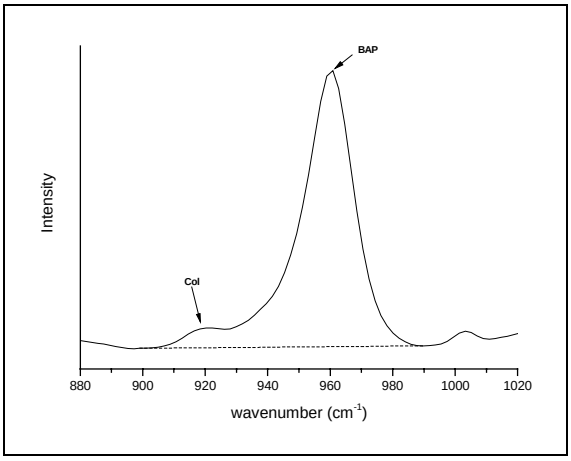

Figure 2. Morphology of the peak at 961 cm^{-1} corresponding to BAP that is overlapping with the 920 cm^{-1} collagen. The dash line indicates the calculated integrated area.

Equations (1)-(3) can be transformed to:

$$\frac{I^{961}}{I^{j}_{COL}} = \frac{K^{961}_{BAP} + K^{961}_{COL}}{K^{j}_{COL}} \cdot \frac{X_{BAP}}{X_{COL}} \quad \Rightarrow \quad \boxed{\frac{I^{961}}{I^{j}_{COL}} = \frac{K^{961}_{BAP}}{K^{j}_{COL}} \cdot \frac{X_{BAP}}{X_{COL}} + \frac{K^{961}_{COL}}{K^{j}_{COL}}} \quad (4)$$

and

$$\frac{A^{961}}{A^{j}_{COL}} = \frac{K^{961}_{BAP} + K^{961}_{COL}}{K^{j}_{COL}} \cdot \frac{X_{BAP}}{X_{COL}} \quad \Rightarrow \quad \boxed{\frac{A^{961}}{A^{j}_{COL}} = \frac{K^{961}_{BAP}}{K^{j}_{COL}} \cdot \frac{X_{BAP}}{X_{COL}} + \frac{K^{961}_{COL}}{K^{j}_{COL}}} \quad (5)$$

where X_{BAP} and X_{COL} are the mass fraction of BAP and collagen respectively and $X_{BAP}+X_{COL}=100$. Indicator j corresponds to the 1667 cm^{-1}, if the peak of amide I is used and to the 2937 cm^{-1} if the peak of CH_2 vibration is used. From equations (4) and (5) it is expected that intensities ratios or integrated areas ratios are linearly correlated to the ratio of mass fraction of BAP and collagen.

Totally, four calibration lines were created: Two using the peaks at 961 cm^{-1} and 2937 cm^{-1} (intensity height and area) and two using the peaks at 961 cm^{-1} and 1667 cm^{-1} (intensity height and area).

Validation of the calibration curves

Only three of the repetitive spectra were used for the construction of the calibration curve. The rest comprised a test set for the validation of the methodology.

For each calibration curve ten standard samples were used. Some samples appear to deviate from the straight line so they were considered as outliers and extracted from the model. In order to evaluate the effectiveness of this extraction in terms of predictability of the model, the following parameters were compared:

$$RMSEE = \sqrt{(X_{std} - \hat{X}_{std})^2 / (N-2)} \quad (6)$$

$$RMSEP = \sqrt{(X_{obs} - X_{pred})^2 / N_t} \quad (7)$$

where RMSEE= root mean square error of estimation and RMSEP=root mean square error of prediction, X_{std} is the % mass fraction of the mixtures used for the creation of the calibration line, $\hat{X}_{std}$ is the corresponding % mass fraction predicted by the model for the above mixtures, X_{obs} the known % mass fraction of a test sample, X_{pred} the % mass fraction predicted by the model for the test sample, N the number of the calibration samples and N_t the number of samples in the test set. Obviously, the smaller the values of RMSEE and RMSEP the better the calibration model is.

Implementing the above statistical tests to our calibration models it was found that the best models were the following:

Using intensity (heights)

$$\frac{I^{961}}{I^{2397}_{COL}} = 0.2963 \cdot \frac{X_{BAP}}{X_{COL}} + 0.2103 \quad (8)$$

N	S_m	S_b	SD	R	RMSEE
8	0.00845	0.04401	0.056	0.998	1.449

$$\frac{I^{961}}{I^{1667}_{COL}} = 1.5707 \cdot \frac{X_{BAP}}{X_{COL}} + 0.2597 \quad (9)$$

N	S_m	S_b	SD	R	RMSEE
9	0.4062	0.0634	0.6226	0.994	0.954

Using integrated intensities (area)

$$\frac{A^{961}}{A^{2397}_{COL}} = 0.0611 \cdot \frac{X_{BAP}}{X_{COL}} + 0.0764 \quad (10)$$

N	S_m	S_b	SD	R	RMSEE
8	0.00199	0.01036	0.01318	0.997	1.449

$$\frac{A^{961}}{A^{1667}_{COL}} = 0.3889 \cdot \frac{X_{BAP}}{X_{COL}} + 0.3343 \quad (11)$$

N	S_m	S_b	SD	R	RMSEE
7	0.00607	0.04176	0.05848	0.999	0.673

where N: number of calibration samples used, S_m: standard deviation of the slope, S_b: standard deviation of the intercept, SD: standard deviation about regression and R: correlation coefficient.

The validation of the above curves was accomplished by means of the test set. In particular, the equations (8)-(11) were used to predict the values of X_{BAP} for known samples and afterwards RMSEP was calculated from equation (7). The 95% confidence intervals were also calculated for each one of the ten test samples. Table 1 summarizes the values for RMSEP and mean confidence interval (C.I.) for all the ten samples.

Table 1. *RMSEP and mean confidence interval (C.I.) for the ten samples of the test set, for each calibration curve.*

Equation	RMSEP	Mean C.I.
(8)	**1,132**	**8,93**
(9)	**0,965**	**16,22**
(10)	**1,056**	**10,22**
(11)	**1,252**	**6,99**

Chemometric approach

Although the accuracy of the above models is quite good, the precision is under debate because the confidence intervals are large. Thereupon, a chemometrical approach of the Raman data was attempted. The SIMCA-P 11 software of Umetrics was used for chemometrical analysis. Partial least square (PLS) was the method applied for the quantification of BAP and collagen. In particular, the same methodology as before was followed. From the six repetitions those with odd number were used for the construction of the calibration model and the even repetitions comprised the test set. In PLS the whole spectrum could be used but in our case we found that optimal results came up using Raman data in the range 350 -1800 cm^{-1}.

Spectral filters (mathematical functions for signal correction) provided by SIMCA were implemented in order to improve our model. Indeed, testing various spectral filters it was found that *standard normal variate* (SNV) provided the best results. Specifically, the model had one principal component and gave R^2=0.997 and Q^2=0.997, where R^2 represents the correlation coefficient of the fitted line and Q^2 the predictive ability of the model (the closer to the unity the better the predictive ability of the model0. RMSEE and RMSEP were found to be 0.649 and 0.920, respectively. Although these values are not significantly different from the calibration models described by equations 8-11 the mean confidence interval for the test set was only 0.172, demonstrating a superior precision for the chemometric model.

CONCLUSION

All the calibration models derived are characterized by small values of RMSEE and RMSEP, showing good fitting and prediction ability. The chemometric model yielded the best RMSEP but not very different from the respective values of the other models. In addition, the chemometric model found to be more precise since it exhibited very low mean confidence interval 0.172, significantly lower than the other models.

BIBLIOGRAPHY

[1] R. Marcus, D. Feldman, D.A. Nelson, C.J. Rosen, *"Osteoporosis"*, Third Edition-Volume I, Academic Press 2007.

[2] J. M. Burnell, D. J. Baylink, C. H. Chestnut, 3rd, M. W. Mathews, and E. J. Teubner. *Bone matrix and mineral abnormalities in postmenopausal osteoporosis*. Metabolism, 31 (1982) 1113–1120.
[3] K. I. Kivirikko. *"Collagens and their abnormalities in a wide spectrum of diseases"* Ann Med 25 (1993) 113-126.

[4] C. Krafft, V. Sergo, *"Biomedical applications of Raman and infrared spectroscopy to diagnose tissues"* Spectroscopy 20 (2006) 195-218.

[5] E. R. C. Draper , M. D. Morris, N. P. Camacho, P. Matousek, M. Towrie, A. W. Parker, A. E. Goodship, *"Novel assessment of bone using time-resolved transcutaneous Raman spectroscopy"*, Journal of Bone and Mineral Research 20 (2005) 1968-1972.

[6] P. Moran, M. R. Towler, S. Chowdhury, J. Saunders, M. J. German, N. S. Lawson, H. M. Pollock, I. Pillay, D. Lyons, *"Preliminary work on the development of a novel detection method for osteoporosis"*, Journal of Materials Science-Materials in Medicine, 18 (2007) 969-974.

[7] D. Bettin, J. Polster, V. Rullkotter, R.von Versen and S. Fuchs, "*Good preservation of initial mechanical properties in lipid-extracted, disinfected, freeze-dried sheep patellar tendon grafts*", Acta Orthopaedica Scand., 74 (2003) 470-475.

[8] N. Kaku, H. Tsumura, M. Kataoka, H. Taira and T. Torisu, *"Influence of aeration, storage, and rinsing conditions on residual ethylene oxide in freeze-dried bone allograft",* Journal of Orthopaedic Science, 7 (2002) 238-242.

[9] J. D. Termine, E. D. Eanes, D. J. Greenfie, M. U. Nylen, R. A. Harper, *"Hydrazine-deproteinated bone mineral - physical and chemical properties", Calcified Tissue Research,* 12 (1973) 73-90.

[10] A. J. Bailey, S. F. Wotton, T. J. Sims and P. W. Thompson, "*Post-translational modifications in the collagen of human osteoporotic femoral head*", Biochemical and Biophysical Research Communications, 185 (1992) 801-805.

[11] H. Oxlund, Li. Mosekilde and G. Ortoft, "*Reduced concentration of collagen reducible cross links in human trabecular bone with respect to age and osteoporosis*", Bone, 19 (1996) 479-484.

[12] K.M. Shah, J.C.H. Goh, R. Karunanithy, S.L. Low, S.Das De and K. Bose, *"Effect of decalcification on bone mineral content and bending strength of felin femur",* Calcified Tissue International, 56 (1995) 78-82.

[13] D. R. Eyre and M. J. Glimcher, "*The dissolution of bovine and chicken bone collagens in concentrated formic acid",* Calcified Tissue Research, 15, (1974) 125-132.

[14] D. Strommen, K. Nakamoto, Laboratory Raman Spectroscopy, Wiley, New York, 1984, p. 71.

[15] M. D. Morris, W. F. Finney, "*Recent developments in Raman and infrared spectroscopy and imaging of bone tissue"*, Spectroscopy 18 (2004) 155-159.